Transfer Functions and Seismic Discrimination: A KNET Case Study

Marie D. Renwald [1]
Steven R. Taylor
Terry C. Wallace[1]

Los Alamos National Laboratory
Los Alamos, NM 87545

[1] Also at University of Arizona

LA-UR-02-7658

December 12, 2002

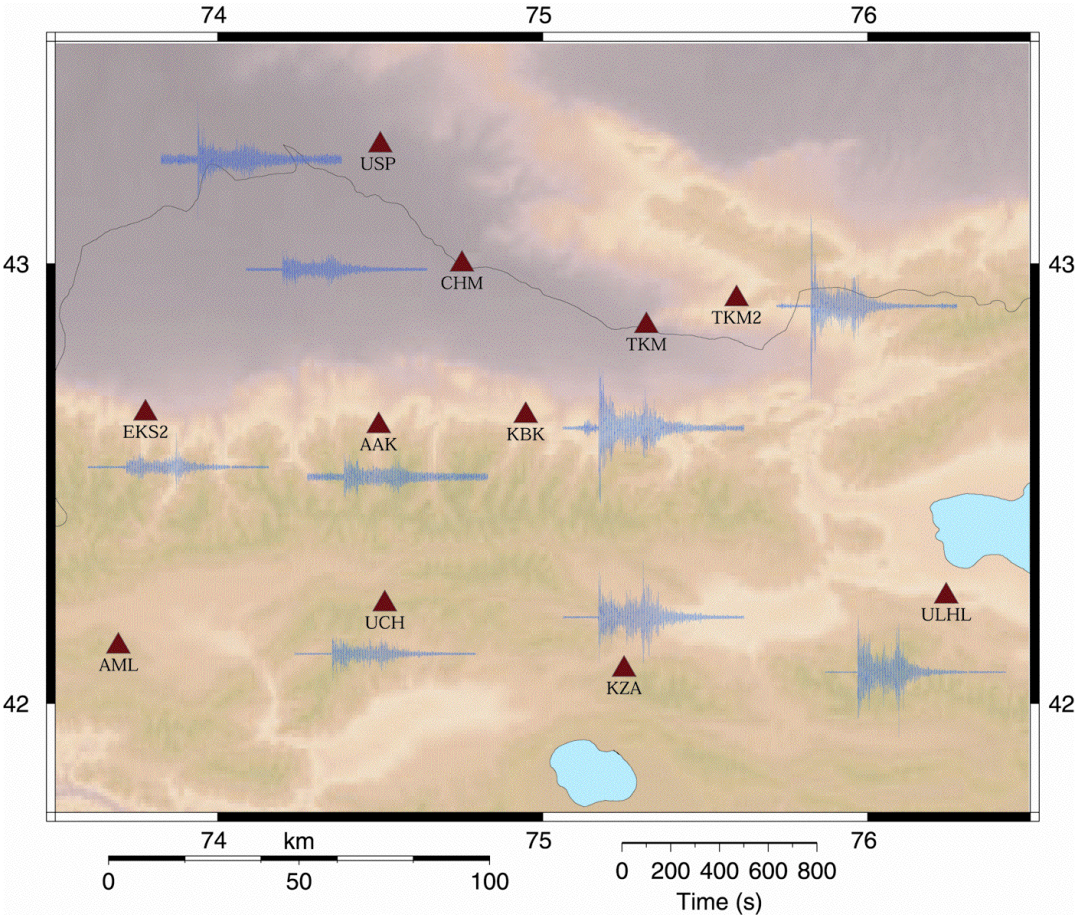

ABSTRACT. The basic challenge of monitoring any nuclear testing moratorium lies in quantitatively identifying earthquakes from explosions. The problem is best characterized as finding small explosions, potentially tested clandestinely; the small size requires using regional distance (< 1500 km) seismic recordings. However, regional seismograms can show both great complexity due to the crust-mantle waveguide and great variability for different source-station paths. To effectively develop regional discriminants at any given station requires a ground-truth database consisting of waveforms from both earthquakes *and* explosions. Newly installed stations in official monitoring networks lack such a database, which severely affects confidence in successfully discriminating between different types of events. To address this problem, we have investigated a procedure to predict a discriminant at a newly installed seismic station using the actual discriminant at a long operating station and a transfer function for that specific station pair.

The dataset consists of six explosions and nine earthquakes at or within 100 km of the Lop Nor Chinese nuclear test site and recorded at the ten-station, very broadband KNET network in Kyrgyzstan. We have predicted four discriminants (two phase ratio and two cross spectral ratio) using transfer functions for all possible station combinations. Initial results show nearly 1:1 correlation (for three of four discriminants) between the discriminant predicted with a transfer function and the actual discriminant recorded at each station. We also investigated what role interstation distance plays in the success of the prediction; F-statistics suggest that interstation distance does not affect the prediction. This implies that we need not necessarily use close-by stations to effectively predict discriminants at stations that have never recorded an explosion.

Introduction

To effectively monitor a nuclear testing moratorium requires accurate detection, location, and identification of explosions from a background natural seismicity. Although fundamental source physics can predict expected differences between earthquakes and explosions, experience indicates that discriminating between explosions and earthquakes is highly dependent on source and station location. This is particularly true for recordings at regional distances; seismograms

can be quite complex due to wave behavior at the crust-mantle waveguide as well as due to the variability in differing source-station paths. As new stations are installed in official monitoring networks (such as the IMS), the lack of recording history can dramatically affect confidence in discrimination. While some of the monitoring stations have established recording histories, many have never recorded a nuclear explosion. To address this problem, we investigate the use of transfer functions to predict explosion characteristics at newly installed stations using the explosion characteristics from long operating stations.

Historical work has focused on transporting regional discriminants between different tectonic regions (Baumgardt and Der, 1994); however, no studies have been done to address the specific problem of using a historical station to calibrate a newly-installed seismic station. The problem can be approached by considering the data available for both new and historical stations in terms of the frequency domain. For a given event, each station will produce an amplitude spectrum which is composed of a source spectrum, earth response, and site response. The goal is to predict the amplitude spectrum for an explosion at a new station by using a transfer function and the explosion spectrum for a historical station. We have developed a procedure to simply compute transfer functions using known effective regional spectral discriminants (Hartse *et al.*, 1997) for a database of earthquakes and explosions located near the Lop Nor nuclear test site in western China and recorded at the KNET array in Kyrgyzstan. We then tested this procedure by first predicting explosions at the KNET array and then evaluating our predictions against the actual data recorded there.

Transfer Functions

The goal of simulating the expected explosion characteristics at a newly installed seismic station requires a transfer function which is composed of three filter functions: (1) a source excitation function which accounts for the explosion spectral effects, (2) a propagation filter which accounts for the effects of crustal and mantle structure on the partitioning of seismic energy as well as focusing and attenuation effects, and (3) a site response.

We can account for these filter functions by using the frequency domain model for seismic wave generation and propagation. The amplitude spectrum between a given source, *i*, and receiver, *j*, is given by

$$A_{ij}(\omega) = S_i(\omega)E_{ij}(\omega)P_j(\omega) \tag{1}$$

where *S* is the source-excitation spectrum, *E* is the Earth response, and *P* is the site response. Letting $i = X,Q$ for explosion, earthquake, respectively and $j = S,O$ for surrogate and operational station, respectively, we can write three equations representing the data that will be available for calibrating a new station

$$\begin{aligned} A_{QS}(\omega) &= S_Q(\omega)E_{QS}(\omega)P_S(\omega) \\ A_{QO}(\omega) &= S_Q(\omega)E_{QO}(\omega)P_O(\omega) \\ A_{XS}(\omega) &= S_X(\omega)E_{XS}(\omega)P_S(\omega) \end{aligned} \tag{2}$$

and we wish to predict what the explosion spectra will look like at the operational station

$$A_{XO}(\omega) = S_X(\omega)E_{XO}(\omega)P_O(\omega) \tag{3}$$

For a common source (assume a well-recorded earthquake for this example) recorded at both *S* and *O*, we wish to predict the explosion characteristics at *O*. In this study, the calibration earthquake is within 100 km of the area being monitored (varying this parameter is a topic which requires further study). Computing a spectral ratio for the calibration earthquake recorded at *S* and *O* (using equation 2)

$$\frac{A_{QO}(\omega)}{A_{QS}(\omega)} = \frac{E_{QO}(\omega)P_O(\omega)}{E_{QS}(\omega)P_S(\omega)} = T_Q(\omega) \tag{4}$$

so

$$A_{QO}(\omega) = T_Q(\omega)A_{QS}(\omega) \tag{5}$$

Similarly,

$$\frac{A_{XO}(f)}{A_{XS}(f)} = \frac{E_{XO}(f)P_O(f)}{E_{XS}(f)P_S(f)} = T_X(f) \tag{6}$$

and

$$A_{XO}(f) = T_X(f)A_{XS}(f) \tag{7}$$

Noting that we do not actually have $A_{XO}(f)$, we can predict it with

$$A_{XO}(f) = T_Q(f)A_{XS}(f) \tag{8}$$

In this study, we consider the validity of using equation (8) for predicting explosion characteristics at newly-operational seismic stations, and the associated limitations and errors. In doing so, we are essentially asking is $T_X(f) = T_Q(f)$? From equations (4) and (6) we have

$$\frac{E_{XO}(f)P_O(f)}{E_{XS}(f)P_S(f)} = \frac{E_{QO}(f)P_O(f)}{E_{QS}(f)P_S(f)} \tag{9}$$

thus, we are assuming

$$\frac{E_{XO}(f)}{E_{XS}(f)} \approx \frac{E_{QO}(f)}{E_{QS}(f)} \tag{10}$$

One issue that we must be concerned with is how to best address propagation and source effects on the amplitude spectra of our observed data. Typically, the MDAC method is employed to reduce these effects and improve discrimination performance (Taylor *et al.*, 2002). In this study, for simplicity, we have used discriminant ratios instead of amplitudes. Based on the results of

this simpler case, future work will focus on using MDAC-corrected amplitudes to compute and test transfer functions.

Data and Data Processing

The data set consists of six nuclear explosions (**Table 1**) detonated at the Lop Nor test site in western China, and nine earthquakes within 100 km of Lop Nor (**Figure 1**). These data were recorded at the Kyrgyzstan Seismic Network (KNET) (**Figure 2**); the three component broadband (BH) data was downloaded from the IRIS Data Management Center (DMC). KNET has been operational since September 1991 and features ten Streckeisen STS-2 sensors. Seismic data at KNET is very broadband (0.008 – 40 Hz) and as of 1994, triggered data records at 100 samples/sec and continuous data at 40 samples/sec.

The KNET array was chosen for several different reasons: first, the array is at a regional distance from the Lop Nor test site (~1200 km) , so we can utilize regional discriminants that have been proven successful in western China (Hartse *et al.*, 1997); second, the KNET stations have recorded a number of earthquakes and explosions (**Table 2**); third, a wide range of interstation distances (~40 – 200 km) will allow us to determine what effect, if any, the role interstation distance plays in the success of the transfer functions. Finally, KNET is situated in a geologically diverse environment (within both the Tien Shan mountains and the Kazakh platform) featuring a complex series of thrust faults. This allows us to investigate how variable topography and geology affect the success of predicting a discriminant at one station using the discriminant at a station in a different geologic setting. **Figure 3** shows an example of the variability in waveforms seen at KNET - the July 29, 1996 nuclear explosion at Lop Nor was recorded at nine stations. Stations to the right of KBK show very strong P and surface wave energy (as compared to stations to the left of KBK).

After the data were downloaded, deglitching was done using SAC. The regional phases Pn, Pg, Sn, and Lg were picked using the procedure outlined in Hartse (2001) based upon a velocity model in Hartse (2001). Instrument corrections were made using response files downloaded from the DMC; all data was instrument corrected into ground velocity. **Figure 4** illustrates instrument

corrected waveforms for four KNET stations for a 1996 explosion and a 1999 earthquake. Both unfiltered data and data filtered in the 6 to 8 Hz pass band are shown.

Pseudo-spectral displacement measurements were then made utilizing several custom Matlab-based programs and functions. Event and pick information stored in SAC headers was loaded into Matlab. When a Pn pick was made, all other picks were time shifted relative to it (based on the on a velocity model of V_{Pn} = 8.1 km/s (Hartse, 2001)). The mean was removed from the signal and a cosine taper was applied. Next, a bandpass (Butterworth, order 4) filter in each of the six MDAC frequency bands (**Table 3**) was applied to the signal. For each MDAC band, signal, noise and pre-phase noise windows were defined, again using the procedures outlined in Hartse (2001) and RMS velocities were calculated for the signal, noise, and pre-phase noise based upon the appropriate window lengths. Finally, RMS velocities were converted into pseudo-spectral displacement using Parseval's theorem and were also corrected for different window lengths for both the signal and noise measurements (Taylor, 2002). The output contained log amplitude values for each of the six MDAC bands for each regional phase; these amplitudes were then used to calculate discriminants and finally transfer functions.

Predicting a Discriminant with a Transfer Function

Four discriminants were utilized in this study: two phase ratios (Pn4/Sn4 and Pg5/Lg5) and two cross-spectral ratios (Pn4/Sn2 and Pn4/Lg2), where the numbers in each discriminant correspond to the appropriate MDAC frequency band. An initial investigation of each discriminant (**Figure 5**) reveals that three of the discriminants (Pn4/Sn2, Pn4/Sn4, Pn4/Lg2) behave well while Pg5/Lg5 does not. There is little population separation in that discriminant; the other three show a good separation between earthquakes and explosions. Further discussion about the Pg5/Lg5 discriminant at KNET will follow in the *Discussion* section.

Transfer functions were computed for each MDAC band using equations (4) and (6), for earthquakes and explosions, respectively. Transfer functions for all stations predicting all stations for all events were computed. A single transfer function for each surrogate-operational

station pair was calculated by taking the mean of all transfer functions computed for each pair of stations.

Using equations (5) and (7), the four discriminants were predicted using the transfer functions and the observed discriminants at each surrogate station. **Figure 6** illustrates the results of the surrogate station predicting the discriminants for explosions at the operational stations and **Figure 7** shows the predictions for earthquakes at the operational stations. Predictions consist of each surrogate station predicting each operational station; all pairs are considered, so AAK predicting CHM is plotted as is CHM predicting AAK. Additionally, since we have used a mean value for the transfer function, stations predicting themselves are shown. Stations having a phase with a signal to pre-phase noise ratio of less than one are not plotted. For both explosions and earthquakes, we find a good correlation to the 1:1 line, except for the Pg5/Lg5 discriminant, where we see a lot of scatter. This behavior is to be expected given the discriminant's performance at KNET.

The case that is of the most interest, though, is how well the transfer function for the earthquakes predicts explosions. Using equation (8), we predicted the discriminant ratio for explosions (**Figure 8**). We get a good fit to the 1:1 line in all discriminants except for Pg5/Lg5. After having calculated predicted values, we can produce a plot similar to that of Figure 5, showing the discriminant behavior vs. mb (**Figure 9**). Comparing Figure 5 to Figure 9 shows that our predicted discriminants show a slight increase in scatter but still perform well.

One reason for the scatter seen in the predicted discriminants could be due to interstation distance, that is, the proximity of the operational station from the surrogate station. An initial plot of residuals for each discriminant vs. interstation distance (**Figure 10**) appears to show that no such relationship exists. To more quantitatively assess this question, however, we investigated this hypothesis using a regression analysis to compare F-statistics for different regression scenarios.

For the regressions, we assumed the following relationship:

$$y = \beta_0 + \beta_1 x_1 + \beta_2 x_2 \qquad (12)$$

where β_0 represents the mean, x_1 corresponds to the observed discriminant, x_2 is the interstation distance, and ***y*** is the predicted discriminant. The F-statistic can be used to compare a null hypothesis (NH) to an alternative hypothesis (AH) using the residual sum of squares (RSS) and degrees of freedom (d.f.) of each hypothesis. A general form, from Weisberg (1980), is shown in equation (13):

$$F = \frac{(RSS_{NH} - RSS_{AH})/(d.f._{NH} - d.f._{AH})}{RSS_{AH} / d.f._{AH}} \qquad (13)$$

We compared the following situations: (1) NH is our mean (β_0) , AH considers both the mean and observed ratio terms (β_0, β_1) , (2) NH is our mean, AH considers both the mean and interstation distance terms (β_0, β_2) , (3) NH is our mean and observed ratio and AH is the mean, observed ratio, and interstation distance ($\beta_0, \beta_1, \beta_2$) , and (4) NH is our mean and AH is our mean, observed ratio, and interstation distance terms. **Table 4** summarizes the F-statistic for each of the 4 discriminants for each situation. Additionally, the tabulated F value (95% confidence interval) for each discriminant is shown. The cases that we wish to compare are (1) and (3). We want to learn if adding the interstation distance parameter results in an F-statistic value which is greater than the tabulated F. In case (1), the F-statistic is much greater than the tabulated F for each discriminant; in case (2), the F-statistic is not greater than the tabulated F. This result would suggest that adding the distance parameter to equation (12) does not lead to a better fit in the predicted – observed relationship.

Discussion and Conclusions

Utilizing a transfer function to predict discriminants worked well in the three cases (explosions – explosions, earthquakes – earthquakes, and earthquakes – explosions). Comparing the observed values to the predicted values shows general conformity to a 1:1 fit. However, the transfer functions do not seem to work well for the high frequency Pg/Lg discriminant. This is somewhat

surprising considering the success of similar discriminants in western China (Hartse *et al.*, 1997). Examination of MDAC band 5 (6 – 8 Hz) filtered waveforms at AAK (**Figure 4**) may shed some light on this problem. The July 29, 1996 explosion recorded at station AAK, for example, does not exhibit significant difference from the October 18, 1999 earthquake. Compare AAK to station ULHL where the Lg phase for the explosion is very distinctive with respect to the earthquake Lg. The scatter seen in the predicted-observed relationships for the higher frequencies might be due to the poor performance of the discriminant at certain stations. This may be affecting the mean transfer function value used to calculate the predicted ratio, resulting in a poor prediction.

Investigating the question of whether interstation distance plays a role in predicting a discriminant with a transfer function may help to minimize the problem of poorly performing discriminants at certain stations. Multiple regression analysis shows interstation distance does not affect the predicted – observed relationship. This is an important conclusion because it implies we do not need to necessarily use close-by stations to generate transfer functions. Since this is the case, we could use only those stations where certain discriminants perform well to predict those discriminants at other stations.

The success of this work presents a range of future topics to be investigated. First, we would like to employ magnitude and distance amplitude corrections (MDAC) to the data and re-evaluate how transfer functions predict discriminants as well as actual amplitude spectra. This is important because the character of regional distance seismograms is extremely path dependent. In an attempt to calibrate out propagation effects and distortion of the signal due to event size, corrections must be made to the spectral signature. Secondly, we would like to constrain distance scaling effects: for example, how far earthquakes can be from a test site before the transfer functions no longer effectively predict discriminants (or amplitude spectra) at newly-installed stations. In this investigation we used an arbitrary distance of 100 km, resulting in successful predictions; however, placing bounds on this parameter will be important in developing a systematic methodology for calibrating new stations. Similarly, we wish to investigate whether transfer functions calculated using earthquake and explosion data for one tectonic region can be used to effectively discriminate events located in other tectonic regions. This question is crucial

in addressing transfer function variability across different distances and geologic provinces. Finally, a long term goal is to use station MAKZ in Kazakhstan to calibrate discriminants at the newly-installed MKAR array.

Acknowledgements

MDR wishes to acknowledge the NEM group (EES-11) at Los Alamos National Laboratory, specifically Aaron Velasco, who provided initial assistance with regional phase picking; Hans Hartse, who assisted with phase picking and instrument corrections; and George Randall, who provided help with Perl scripting. Additionally, we wish to thank the Incorporated Research Institutions for Seismology (IRIS) Data Management Center for supplying the data used in the project. This work is performed under the auspices of the U.S. Department of Energy by Los Alamos National Laboratory under contract W-7405-ENG-36.

Tables

Table 1 – Earthquakes and Explosions near Lop Nor

Event	*Latitude*	*Longitude*	*mb*
1992-05-21 EX	41.515	88.770	6.5
1993-10-05 EX	41.594	88.686	5.9
1994-10-07 EX	41.600	88.743	6.0
1994-12-26 EQ	41.590	88.830	4.6
1995-08-02 EQ	41.630	88.450	4.1
1995-08-17 EX	41.543	88.837	6.0
1996-03-20 EQ	42.180	87.630	4.8
1996-05-10 EQ	41.870	88.230	3.8
1996-06-08 EX	41.601	88.735	5.9
1996-07-29 EX	41.774	88.392	4.9
1999-01-27 EQ	41.620	88.360	4.5
1999-01-30 EQ	41.670	88.460	5.9
1999-05-01 EQ	42.040	87.960	4.2
1999-05-17 EQ	42.280	87.920	4.2
1999-10-18 EQ	41.770	89.250	5.0

Table 2 – Events recorded at KNET

Event _ Station _	*AAK*	*AML*	*CHM*	*EKS2*	*KBK*	*KZA*	*TKM*	*TKM2*	*UCH*	*ULHL*	*USP*
1992-05-21 EX	x		x	x							x
1993-10-05 EX	x	x	x	x	x		x				x
1994-10-07 EX		x	x	x	x	x			x	x	x
1994-12-26 EQ	x			x				x		x	x
1995-08-02 EQ	x			x	x	x		x		x	x
1995-08-17 EX			x	x	x	x		x		x	x
1996-03-20 EQ	x		x	x	x	x		x	x	x	x
1996-05-10 EQ	x				x	x		x			x
1996-06-08 EX	x		x		x				x		x
1996-07-29 EX	x		x	x	x	x		x	x	x	x
1999-01-27 EQ	x	x		x	x	x		x	x	x	x
1999-01-30 EQ	x	x	x	x	x	x		x	x	x	x
1999-05-01 EQ	x	x		x	x	x		x	x	x	x
1999-05-17 EQ	x	x		x	x	x		x	x	x	x
1999-10-18 EQ	x	x	x	x	x	x	x	x	x	x	x

Table 3 – MDAC frequency bands

MDAC Band	*Frequency Range (Hz)*
1	0.5 - 1.0
2	1.0 - 2.0
3	2.0 - 4.0
4	4.0 - 6.0
5	6.0 - 8.0
6	8.0 - 10.0

Table 4 – F-statistics for linear regressions

	$H_0 : \square_0$ □ $H_1 : \square_0, \square_1$	$H_0 : \square_0$ □ $H_1 : \square_0, \square_2$	$H_0 : \square_0, \square_1$ □ $H_1 : \square_0, \square_1, \square_2$	$H_0 : \square_0$ □ $H_1 : \square_0, \square_1, \square_2$
Pn4/Sn4	29.55	1.30	0.37	14.91
F_tab	2.14	2.11	2.16	2.14
□	□	□	□	□
Pg5/Lg5	32.71	2.98	0.85	16.66
F_tab	1.29	1.29	1.29	1.29
□	□	□	□	□
Pn4/Sn2	262.23	0.54	0.13	129.92
F_tab	1.42	1.42	1.42	1.42
□	□	□	□	□
Pn4/Lg2	437.84	0.01	0.00	217.55
F_tab	1.30	1.30	1.30	1.30

$y = \square_0 + \square_1 x_1 + \square_2 x_2$

y □ predicted ratio

x_1 □ observed ratio

x_2 □ interstation distance

References

Baumgardt, D., Der, Z., Investigation of the transportability of the P/S ratio discriminant to different tectonic regions. SAS-TR-95-60, ENSCO, Inc., Springfield, VA, 1994.

Hartse, H.E., Current Status of LANL Amplitude Measurement Procedures, *Los Alamos National Laboratory*, LA-UR-01-3477, 2001.

Hartse, H.E., S.R. Taylor, W.S. Phillips, and G.E. Randall, Regional event discrimination in central Asia with emphasis on western China, *Bull. Seism. Soc. Am.*, 87, 551-568, 1997.

Hartse, H.E., Regional Phase Arrival Time Picking in Asia, *Los Alamos National Laboratory*, LA-UR-01-3077, 2001.

Taylor, S.R., A.A. Velasco, H.E. Hartse, W. S. Phillips, W.R. Walter, and A.J. Rodgers, Amplitude corrections for regional seismic discriminants, *PAGEOPH*, 159, 623-650, 2002.

Taylor, S.R, Regional Amplitude Measurements, *Los Alamos National Laboratory*, Memorandum, EES-11-02-019, March 25, 2002.

Weisberg, S., Applied Linear Regression, John Wiley & Sons, Inc., 283pp, 1980.

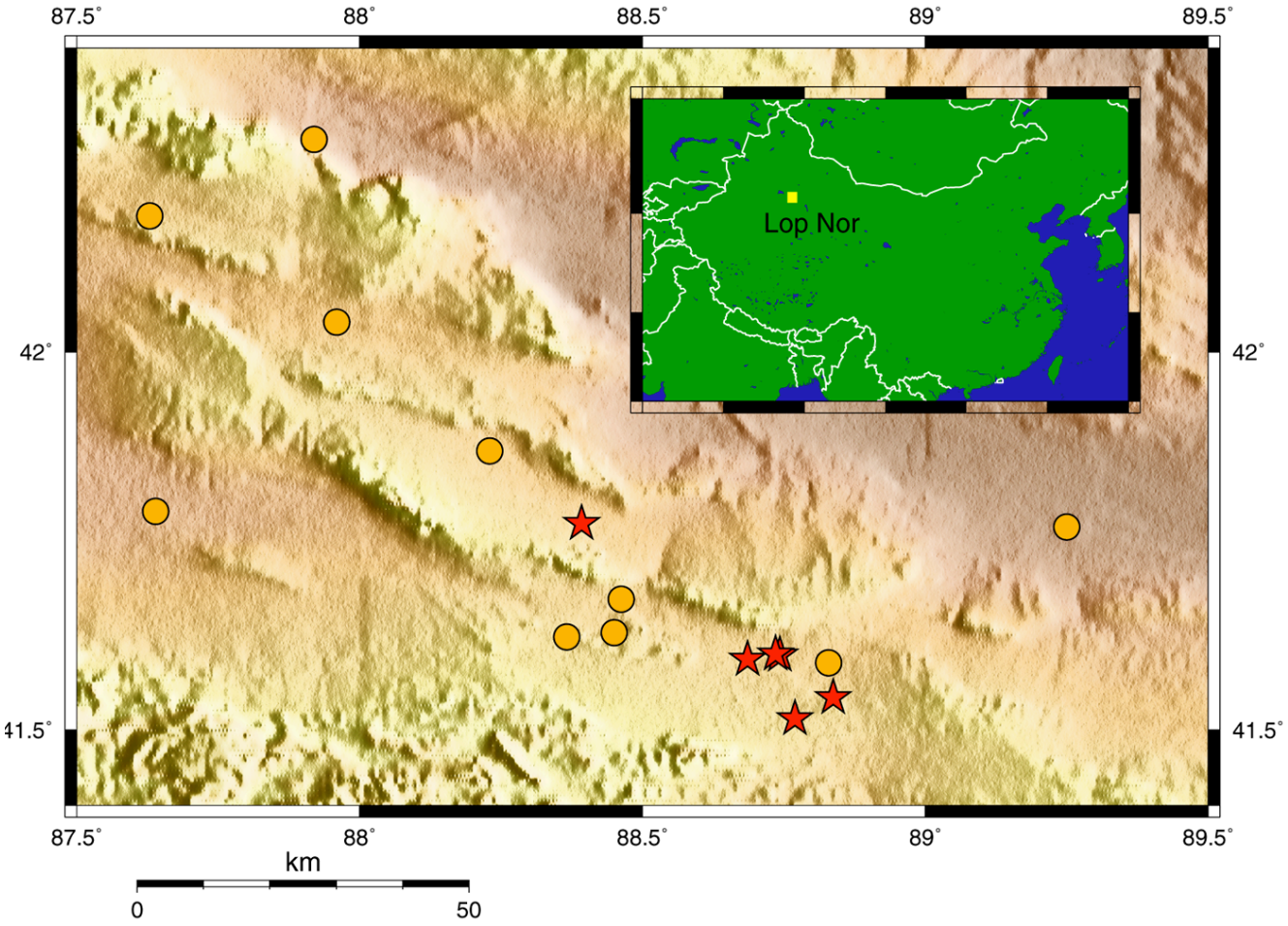

Figure 1: Earthquakes (●) and explosions (★) recorded at the Lop Nor nuclear test site in western China.

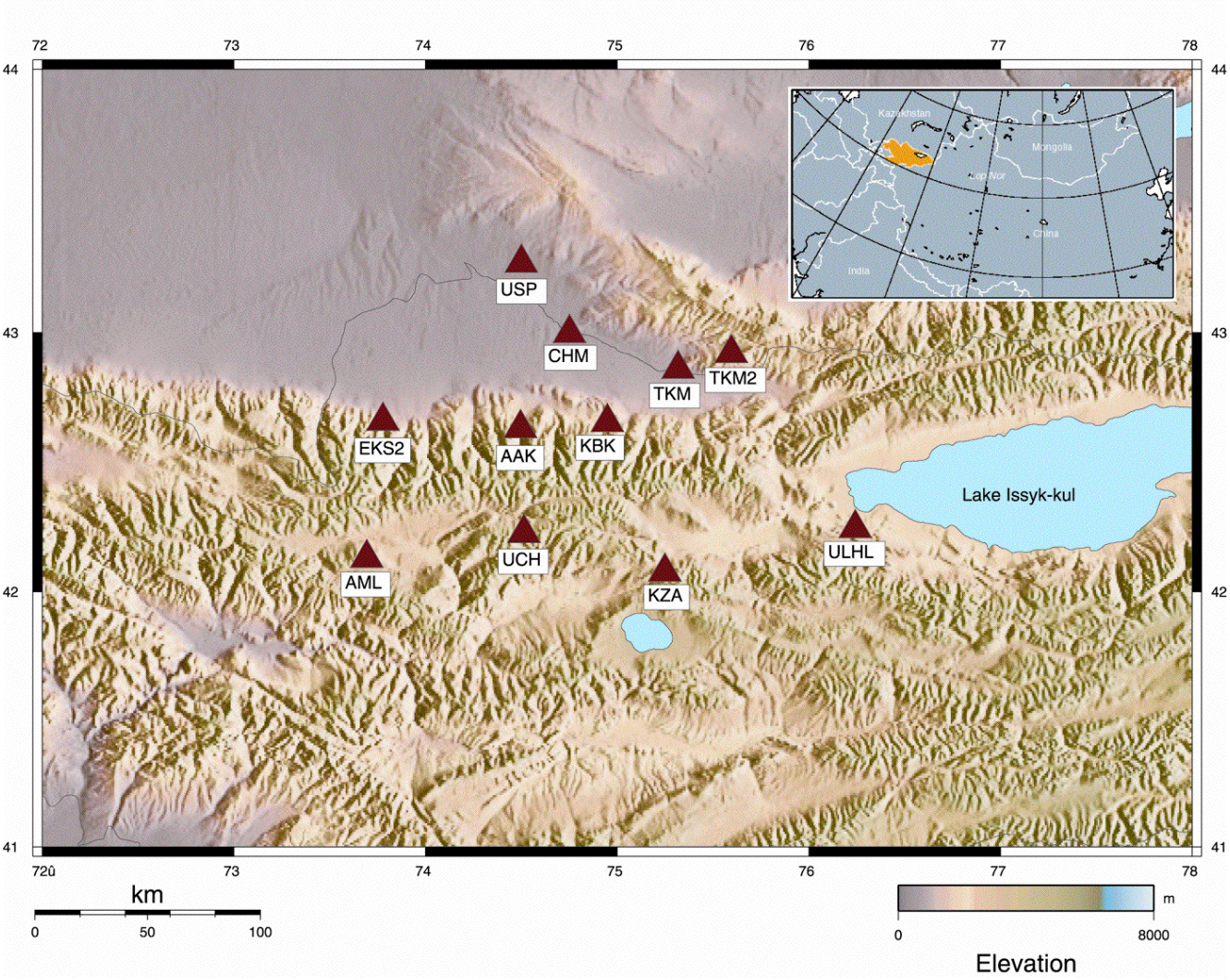

Figure 2: The KNET seismic network located in Kyrgyzstan. The black line represents the border between Kazakhstan and Kyrgyzstan. The inset map highlights the location of Kyrgyzstan (yellow) with respect to other central Asian countries. Note that station TKM was replaced with station TKM2 in 1994.

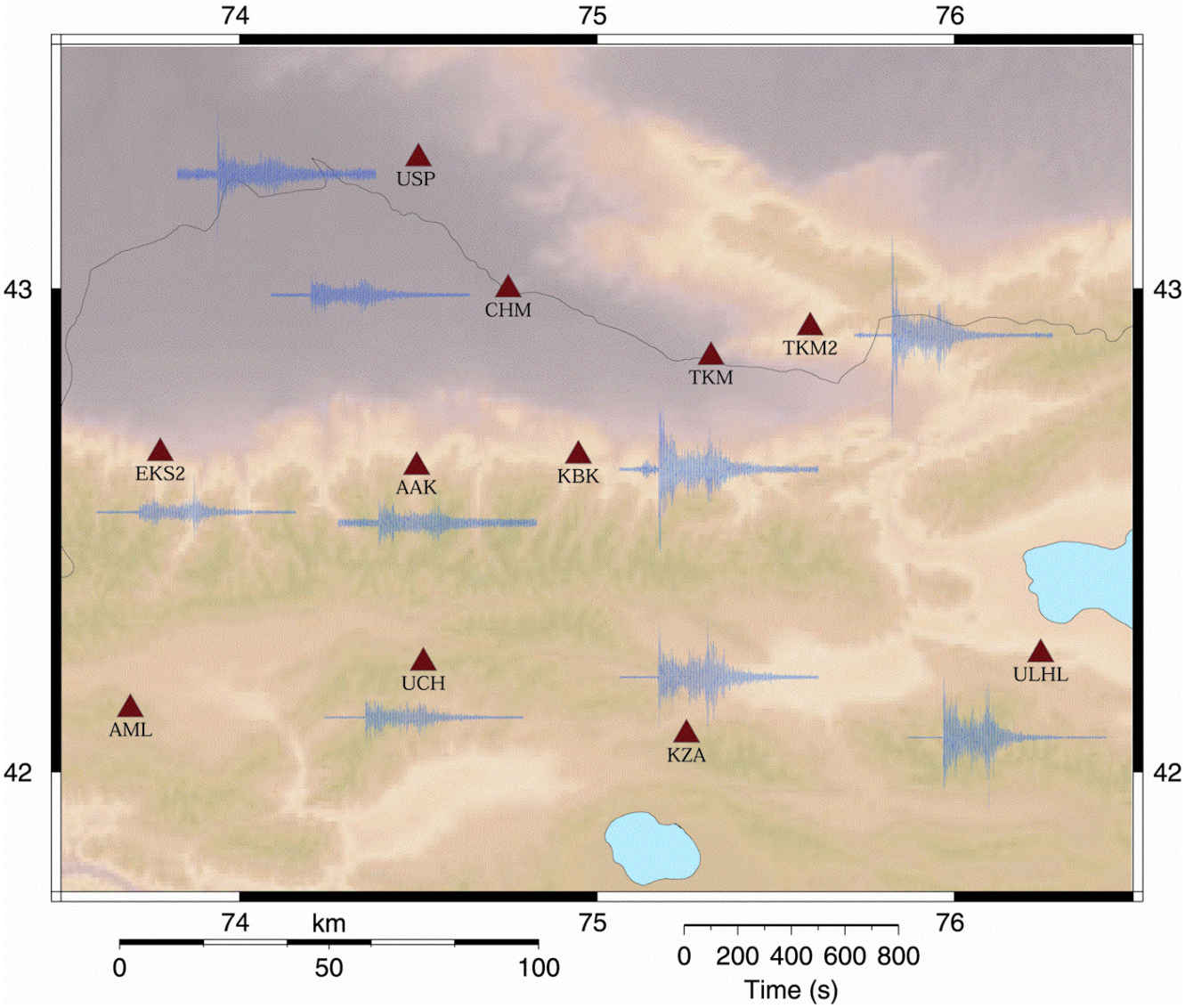

Figure 3: The July 29, 1996 (mb = 4.9) nuclear explosion at Lop Nor recorded at the KNET array. Waveforms show variability which seems to be dependent on a subsurface feature not correlated with topography. Stations to the right of and including KBK have very strong P and surface wave arrivals, while those to left of KBK have much weaker energy. Each waveform is 800 seconds in length and all have the same y-axis scale.

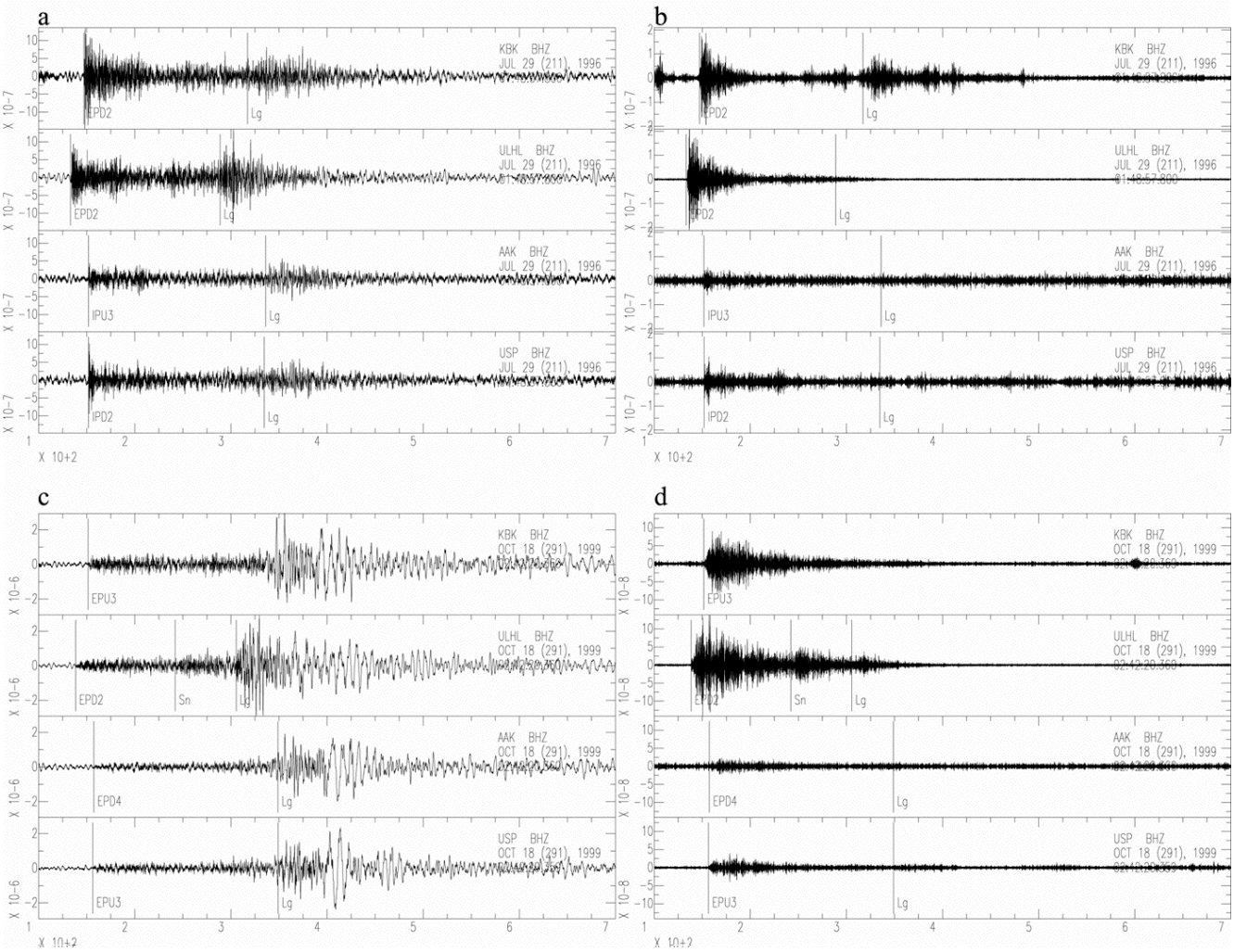

Figure 4 (a,b,c,d): Seismograms for four KNET stations: KBK, ULHL, AAK and USP. An explosion (a, b) (July 29, 1996, mb=4.9) and earthquake (c, d) (October 18, 1999 mb=5.0) are shown for comparison, as are the filtered (b, d) (bandpass 6 to 8 Hz) and unfiltered (a, c) records. Regional phases, when picked, are also shown on the waveforms.

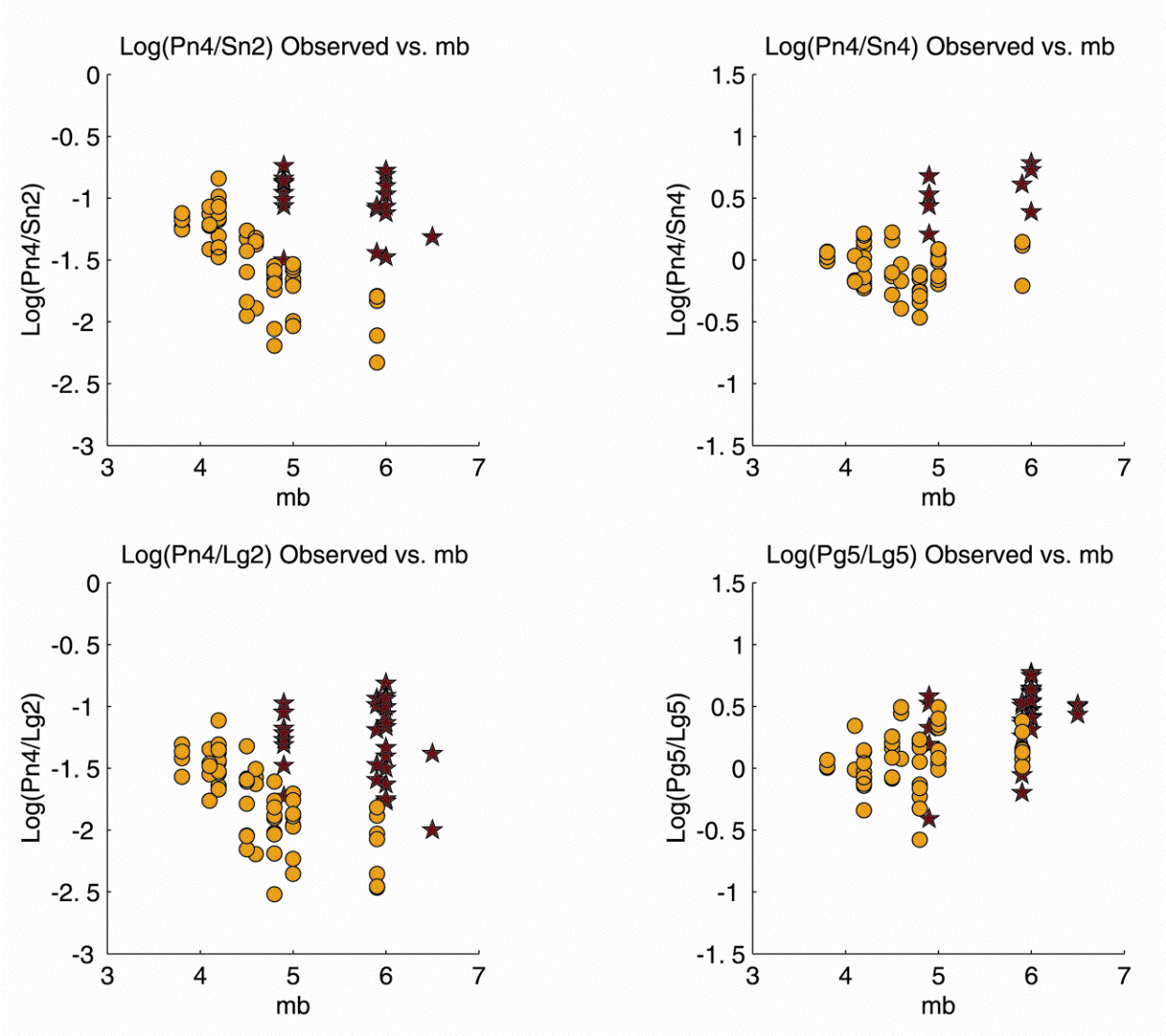

Figure 5: Behavior of the four chosen discriminants recorded at all the KNET stations. The log (discriminant vs. mb) is plotted and events with a signal-to-noise ratio of less than one are not shown.

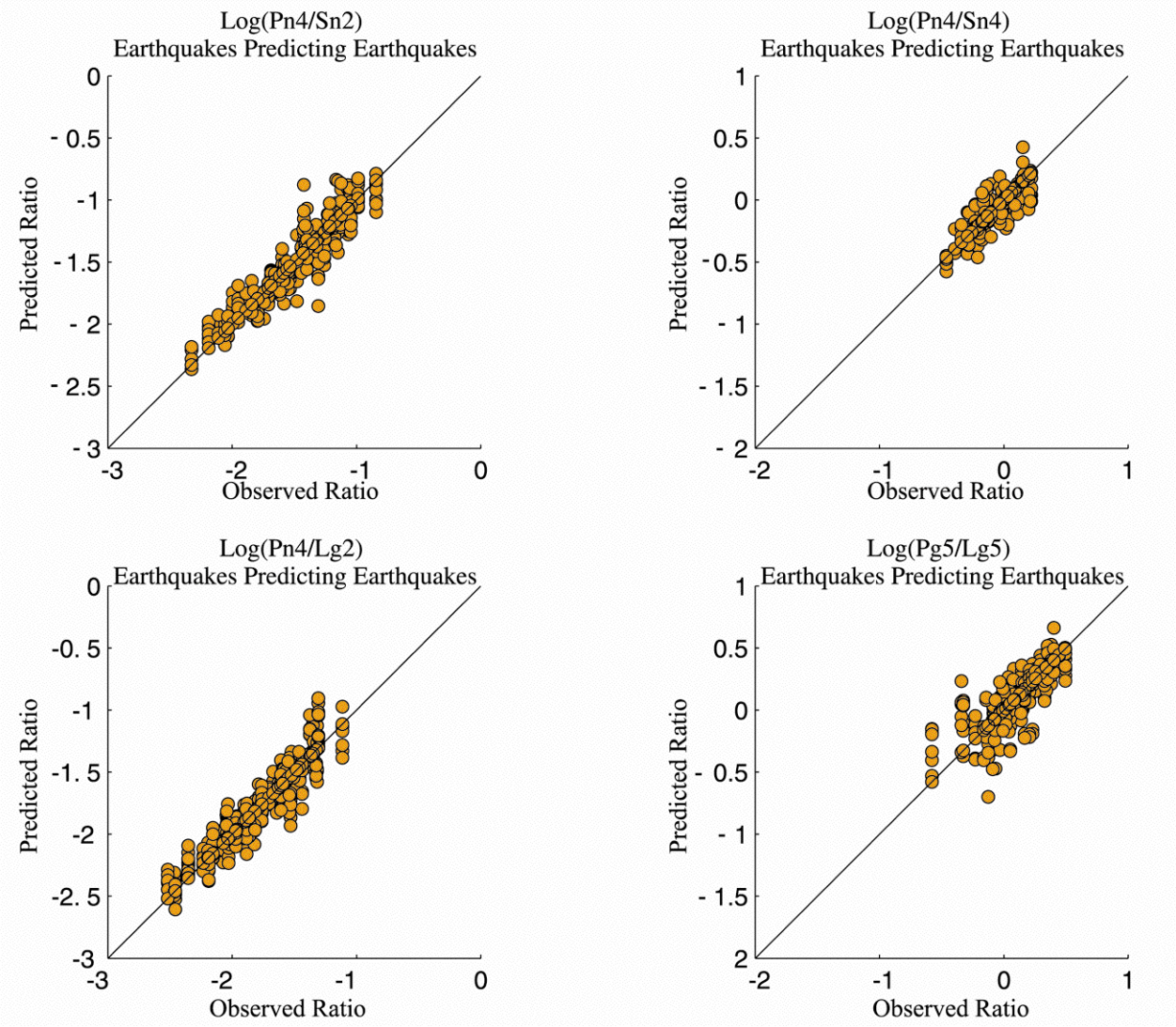

Figure 6: Predicted discriminant vs. observed discriminant (in log space) using the transfer function for explosions to predict explosions. The solid line shows a 1:1 relationship.

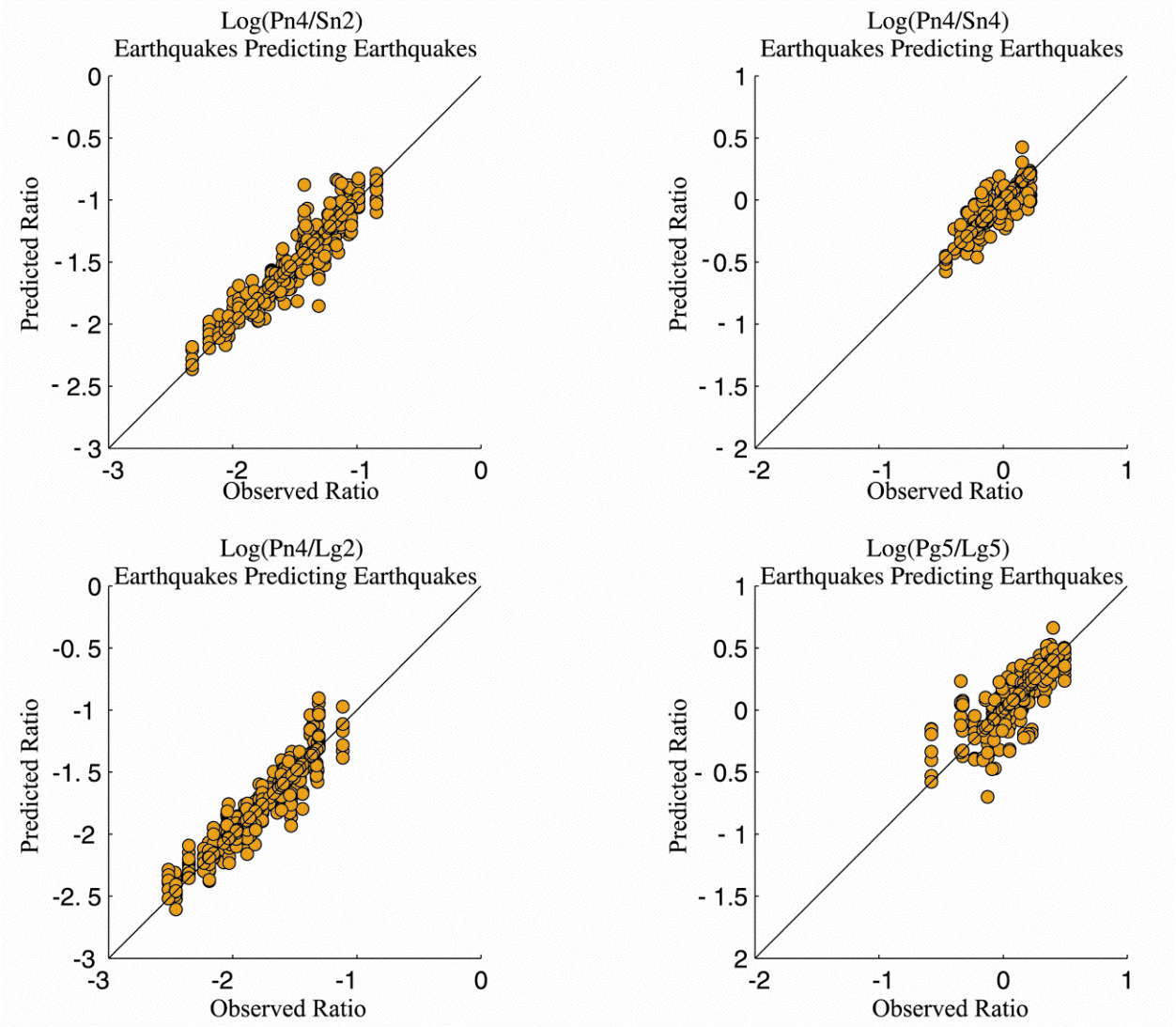

Figure 7: Predicted discriminant vs. observed discriminant (in log space) using the transfer function for earthquakes to predict earthquakes. The solid line, again, shows a 1:1 relationship.

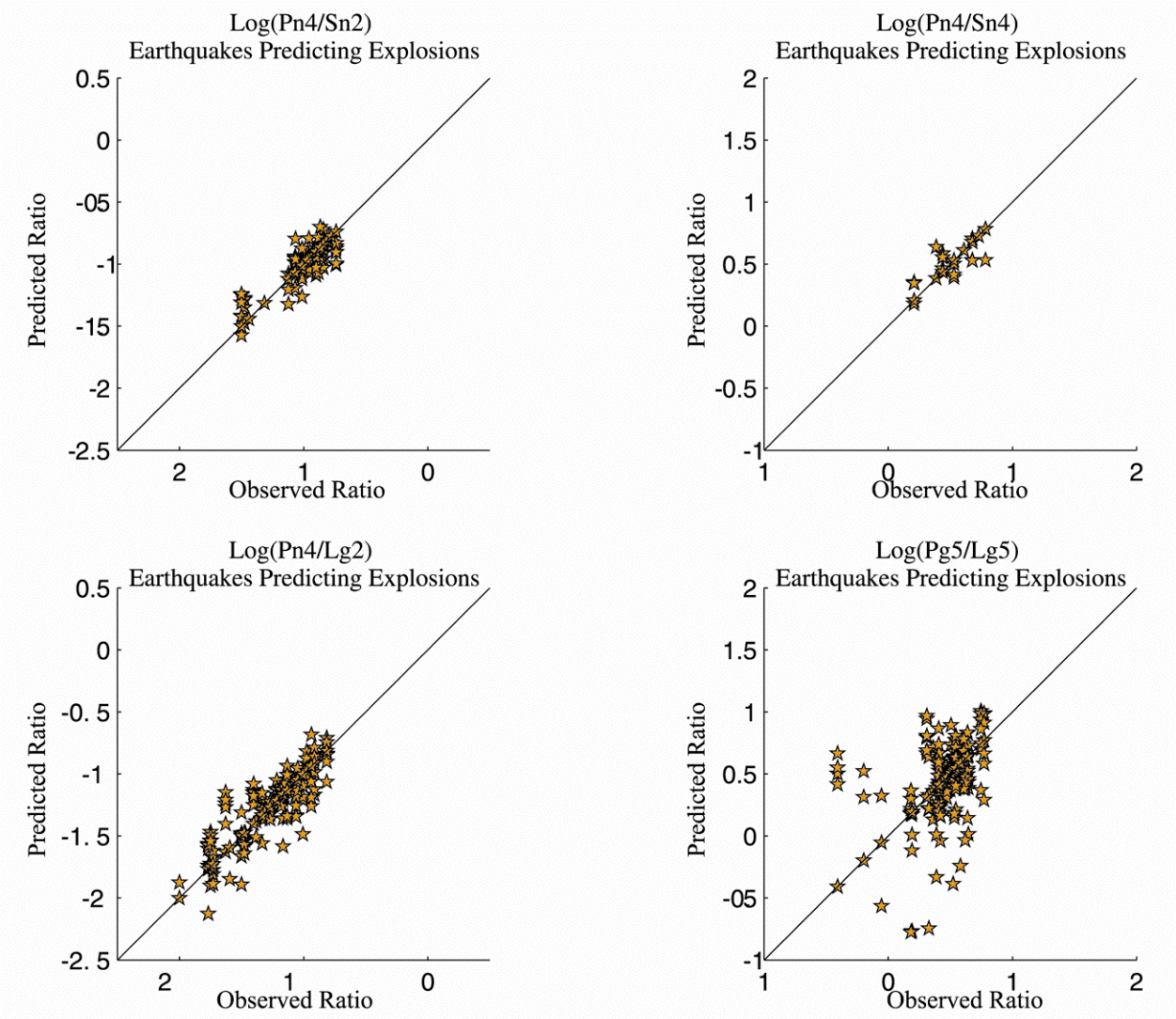

Figure 8: Predicted discriminant vs. observed discriminant (in log space) using the transfer function for earthquakes to predict explosions. The solid line shows a 1:1 relationship.

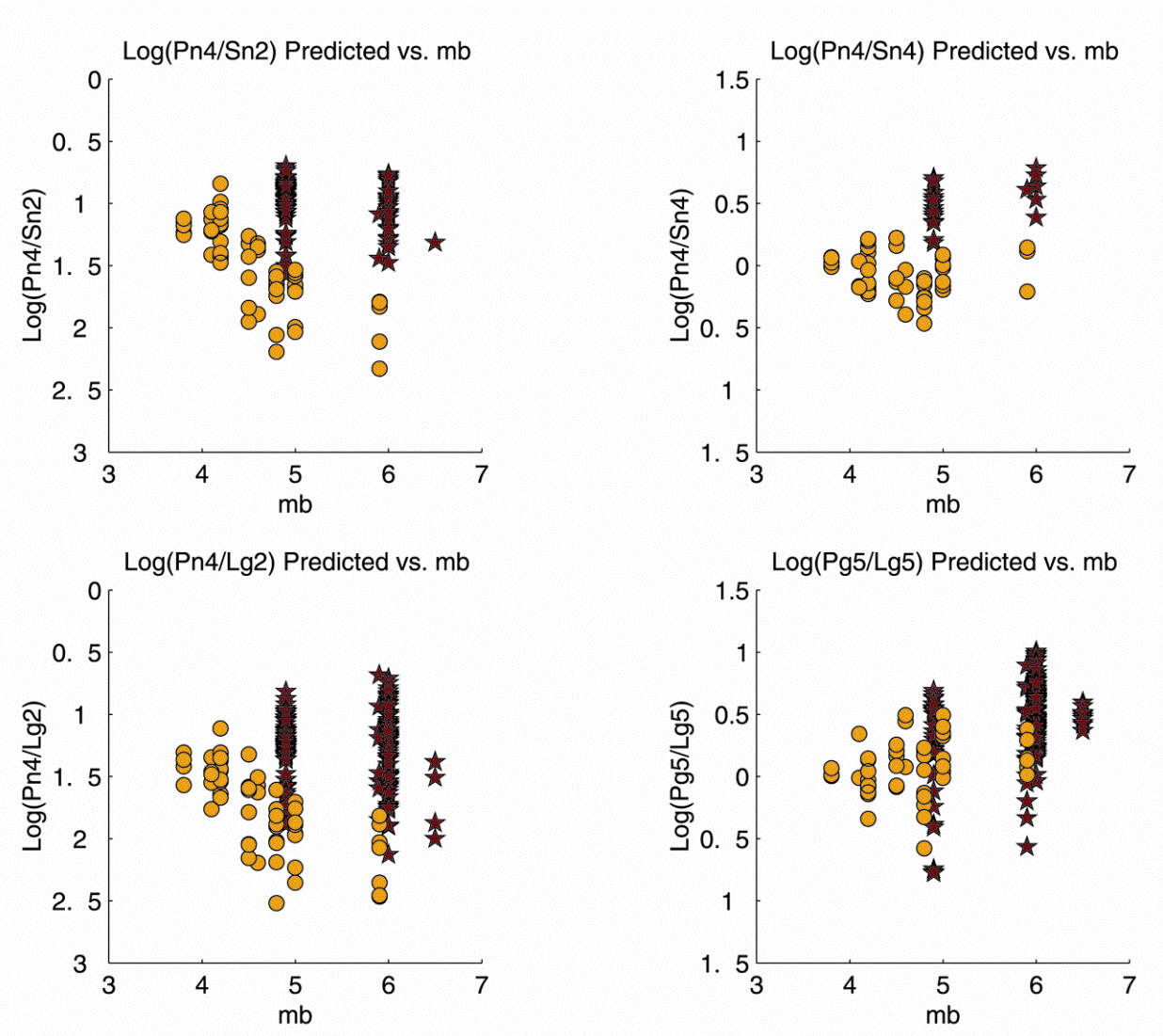

Figure 9: Behavior of the four predicted discriminants recorded at all the KNET stations. The log (discriminant) vs. mb is plotted and events with a signal-to-noise ratio of less than one are not shown.

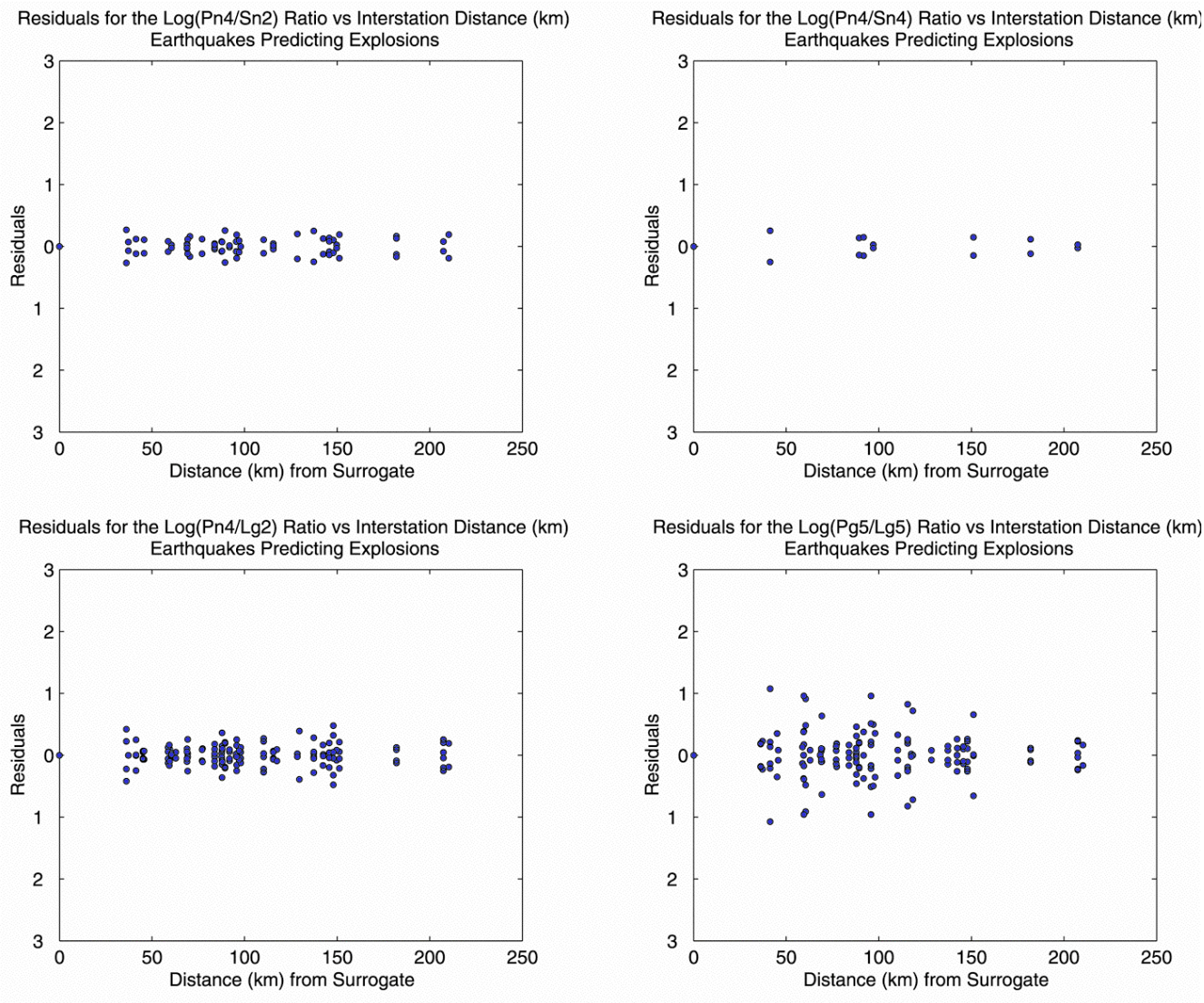

Figure 10: The residuals of the four discriminants vs. interstation distance. Symmetry can be seen due to the fact that station 1 predicting station 2 is calculated, as is station 2 predicting station 1.